

Ontogenetic changes in the internal and external morphology of the ilium in modern humans

Richard Abel¹ and Gabriele A. Macho²

¹Imperial College London, Charing Cross Campus, London, UK

²Institut Català de Paleontologia, Cerdanyola del Vallès, Barcelona, Spain

Abstract

Trabecular architecture forms an important structural component of bone and, depending on the loading conditions encountered during life, is organised in a systematic, bone- and species-specific manner. However, recent studies suggested that gross trabecular arrangement (e.g. density distribution), like overall bone shape, is predetermined and/or affected by factors other than loading and perhaps less plastic than commonly assumed. To explore this issue further, the present cross-sectional ontogenetic study investigated morphological changes in external bone shape in relation to changes in trabecular bundle orientation and anisotropy. Radiographs of 73 modern human ilia were assessed using radiographic and Geometric Morphometric techniques. The study confirmed the apparently strong predetermination of trabecular bundle development, i.e. prior to external loading, although loading clearly also had an effect on overall morphology. For example, the sacro-pubic bundle, which follows the path of load transmission from the auricular surface to the acetabulum, is well defined and shows relatively high levels of anisotropy from early stages of development; the situation for the ischio-iliac strut is similar. However, while the sacro-pubic strut retains a constant relationship with the external landmarks defining the joint surfaces, the ischio-iliac bundle changes its relationship with the external landmarks and becomes aligned with the iliac tubercle only during late adolescence/early adulthood. It is tentatively proposed that the rearrangement of the ischio-iliac strut may reflect a change in locomotor pattern and/or a shift in positional behavior with increasing mass after growth of external bone dimensions has slowed/ceased.

Key words: human iliac growth; ontogeny; trabecular architecture.

Introduction

It is well established that bone formation and remodelling respond to mechanical stimuli: bone is deposited in response to increased strains and resorbed when disused (e.g. Frost, 1990; Lieberman & Crompton, 1998; Carter & Beaupré, 2001). However, rates of bone (re)modelling vary throughout ontogeny and in adulthood. Both rates of growth and cortical drift are highest in infants, and slow considerably from late childhood to late adolescence (Goldman et al. 2009). In adults, increased strain levels will mainly affect bone remodelling towards the medullary cavity, thus leaving external dimensions relatively unaltered (for review, see Ruff et al. 2006); at the microstructural level regional differences in secondary remodelling can provide insights

into the loading history of bones (McFarlin et al. 2008). Clearly thus, an appraisal of adult activity levels from external morphology alone, i.e. without due regard of the internal distribution and structure of bone (e.g. Ruff, 2005), is fraught with problems. In order to overcome these shortcomings in functional morphology, where histological, i.e. destructive, methods are not feasible or desirable, it is now common practice to incorporate some information of internal structures, such as cortical thicknesses of diaphyses (Stock & Pfeiffer, 2001; Marchi et al. 2006; Sládek et al. 2006), trabecular morphology (Ryan & Ketcham, 2002; Ryan & van Rietbergen, 2005; Ryan & Krovitz, 2006; Fajardo et al. 2007) and trabecular arrangement (Biewener et al. 1996; Macchiarelli et al. 1999; Rook et al. 1999; Gefen & Seliktar, 2004), using non-destructive techniques.

Trabecular architecture and organisation is considered particularly informative for the reconstruction of activity patterns within (Agarwal et al. 2004) and between species (Rook et al. 1999; Ryan & Ketcham, 2002; Fajardo et al. 2007), because of the apparently greater potential for remodelling of these structures during adulthood compared with cortical bone (Frost, 1990; Carter & Beaupré,

Correspondence

Gabriele A. Macho, Institut Català de Paleontologia (ICP), Edifici ICP, Campus de la Universitat, Autònoma de Barcelona, Cerdanyola del Vallès, Barcelona 08193, Spain. E: Gabriele.Macho@icp.cat

Accepted for publication 7 January 2011

2001; Kobayashi et al. 2003). This plasticity of trabeculae has long been appreciated in biomechanical studies (Wolff, 1892; Huiskes, 2000; Pearson & Lieberman, 2004; Ruff et al. 2006), and has been investigated with regard to ontogenetic changes (Biewener et al. 1996; Tanck et al. 2001; McColl et al. 2006), ageing (Macho et al. 2005) and activity-related differences (Hou et al. 1990; Lieberman & Crompton, 1998; Iwamoto et al. 1999; Mori et al. 2003; Wallace et al. 2007). However, some recent studies revealed a relatively poor correspondence between locomotor behaviour and trabecular arrangement (Ryan & van Rietbergen, 2005), while experimental ontogenetic studies of the plasticity of trabeculae are equivocal. Mice exposed to different locomotor repertoires during development did not exhibit statistically significant differences in the orientation of trabecular struts (Carlson et al. 2008). Conversely, trabecular alignment in guinea fowl femora was clearly altered following experimentally induced changes in their locomotor repertoire (Pontzer et al. 2006). Whether these contradictory findings are due to differences in experimental set-up or to biological differences in responsiveness of bone between taxa remains unclear. For modern humans, recent evidence suggests a predetermination of some textural properties of the trabecular network, such as the predominant orientation, but plasticity at the microstructural level.

A small cross-sectional study of 15 modern human ilia revealed the characteristic pattern of trabecular bundle orientation to be expressed at about 1 year old (Volpato, 2008). The author tentatively suggested that this could be related to the onset of bipedal locomotion. In toddlers, the pattern of gait is highly unstable however (Ivanenko et al. 2005) and, although it becomes more mature after 4 months of independent walking, it remains more variable than in adults (Hallemans et al. 2005); the adult-like gait parameters are only attained between 5 and 9 years old (Chester et al. 2006). On this basis, functional interpretations for bundle orientation early in life seem unconvincing. Perhaps more significantly, Cunningham & Black (2009a,b) recently showed that an adult-like pattern of trabecular bone density distribution was identifiable even prior to the onset of direct weight bearing. Of course, some mechanical stimulation due to muscle contraction is probable at early stages of development (Delaere et al. 1992; Delaere & Dhem, 1999) and may account for some trabecular structuring, but it is unlikely that the forces thus created are of sufficient magnitude to significantly affect trabecular orientation. The authors therefore invoke genetic influences (ibid.) or patterns of vascularisation (Cunningham & Black, 2010) to account for the observed structuring. At the microstructural level, on the other hand, both Volpato (2008) and Cunningham & Black (2009b) found measures of anisotropy, trabecular thickness and spacing etc., to change in accord with function and age (Tanck et al. 2001; Carlson et al. 2008; Gosman & Ketcham, 2009). Taken together, these findings make it parsimonious to hypothesise that

both bone shape and overall architectural properties are determined early during development (Cunningham & Black, 2009a,b), while microanatomical details may be subject to a greater degree of modification even later in life (Frost, 1990; Carter & Beaupré, 2001; Cunningham & Black, 2009b). To explore this proposition further, the relative timing of cortical and trabecular development was compared in modern human ilia, whereby the orientation and structural properties of the sacro-pubic and ilio-ischial trabecular bundles were assessed in relation to overall bone shape and its changes throughout development (see Berge, 1984, 1998). It was hypothesised that trabecular bundle orientation will retain a constant relationship to external bone shape throughout ontogeny. Ascertaining the relationship between internal and external bony morphology is not only of heuristic value, but will have implications for reconstructing the locomotor behaviour of fossil taxa.

Materials and methods

A cross-sectional ontogenetic series of 73 ilia representing modern humans was studied (Table 1). Unfortunately, sexes were not available for the specimens and could only be assessed in older specimens based on morphological criteria (Scheuer & Black, 2000); the effects of sex were therefore not analysed. Although this is acknowledged to be a confounding factor, it is noteworthy that the sub-adult and adult categories were not biased towards one sex. None of the specimens exhibited any signs of pathology and, where possible, the left ilium was examined. The ilia were assigned to one of five developmental classes based on dental eruption pattern (Penin et al. 2002; Berge & Penin, 2004) and bony fusion (Steudel, 1982; Scheuer & Black, 2000). Adults were defined on the basis of complete epiphyseal fusion (ibid.). The stages are: infants, i.e. no permanent molars erupted; M1s erupted; M2s erupted; sub-adult, i.e. M2/M3 molars erupted, but some epiphyses unfused; adults, i.e. fully erupted teeth and/or fused epiphyses. This corresponds to approximate ages of < 6 years old (infants), 6–12 years old, 12–18 years old, and older; bearing in mind the sample composition (Table 1), variation in the timing of tooth eruption cannot be ruled out.

Landmark data representing cortical morphology were collected directly from bones and from radiographs (Fig. 1; Table 2), while co-ordinate data representing trabecular bundle morphology and textural data of trabecular anisotropy were collected from radiographs. As regards the latter, ilia were radiographed perpendicular to a plane defined by three landmarks: the superior iliac spines (C4, C5) and the posterior apex of the auricular surface (C12). The material housed at the University of Liverpool and Cambridge University was X-rayed using a digital MedCon VG Philips Super 80D CP (Philips Medical Systems, Massachusetts, USA) located at the Alder Hey Children's Hospital (Alder Hey, Liverpool, UK). The Bradford collection was imaged on location using an Acoma DFX-50 (Tokyo, Japan) with AGFA structurix film. Radiographs were taken at a source film distance of 1.2 m, with the axis of the beam centred midway between the iliac spines. Tube voltage varied from 40 to 60 kV, depending on the density of the specimens. The film-based radiographs had a higher resolution and contrast than the digital radiographs. To standardise the data, the radio-

Table 1 Sample size, composition and provenance.

Sample	Age	Developmental stage					Total	Sub-adult & Adult		Provenance
		Infant	M1	M2	Sub-adult	Adult		Male	Female	
Egypt	2040–1997 BC	0	1	6	5	8	20	3	10	Leverhulme Centre for Human Evolutionary Studies, University of Cambridge
Anglo-Saxon	500–1066	3	3	0	0	4	10	3	1	Department of Archaeological Sciences, The University of Bradford
Britain	1066–1450	12	11	4	3	7	37	7	3	Leverhulme Centre for Human Evolutionary Studies, University of Cambridge
Britain	Present day	0	0	0	2	4	6	3	3	Department of Human Anatomy, The University of Liverpool
Total		15	15	10	10	23	73	16	17	

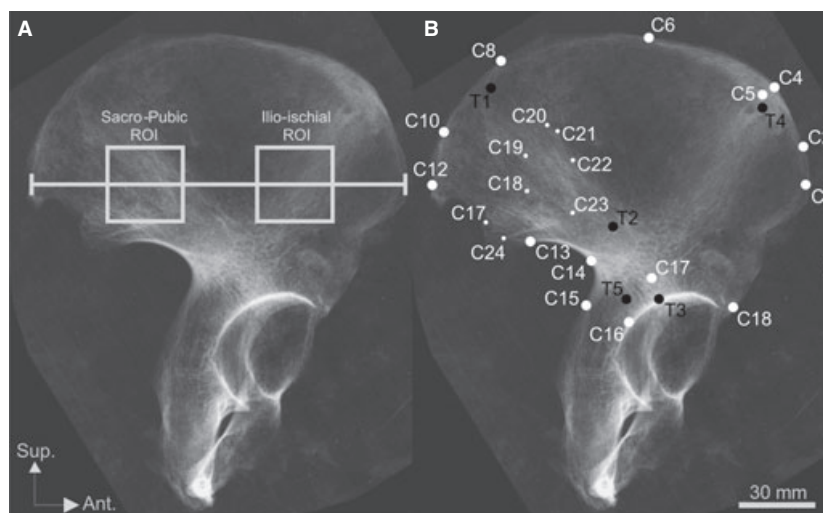


Fig. 1 Radiograph of adult modern ilium illustrating the measurements/landmarks taken. (A) The discrete regions of interest (ROI) from which anisotropy were calculated are highlighted. Although geometrically defined by iliac breadth (i.e. 2/5th and 4/5th of total width), the two areas fall within the confines of the sacro-pubic and ilio-ischial trabecular strut. (B) The landmarks recorded for external shape (white) and internal strut orientation (dark) are shown, and are described in Table 2. White circles denote cortical landmarks, while black circles denote trabecular landmarks. The smaller circles describe the auricular surface.

graphs were all photographed at the same resolution using a Nikon Coolpix 990 camera (Tokyo, Japan). The contrast was normalised by equalising the range between brightest and darkest pixels across radiographs. Prior to data collection the images were converted to 256 grey levels using ImageJ (<http://rsb.info.nih.gov/ij/>). Radiographic measures of the degree of trabecular anisotropy (DA) and landmark-based measures of gross morphology were then collected from the radiographs.

Age-related variation in trabecular micro-architecture was analysed by calculating the DA (Robson-Brown et al. 2002; Martinon-Torres, 2003), which is defined as a measure of how randomly/non-randomly trabeculae are orientated (Whitehouse, 1974; Odgaard, 1997). The DA was calculated for discrete regions of interest (ROI) that were located within the sacro-pubic and ilio-ischial bundles (Fig. 1A). The edges of the square ROI were

scaled to 1/5th of the distance between the superior iliac spines. The sacro-pubic and ilio-ischial ROI were placed, respectively, at 2/5th and 4/5th of the distance between the superior iliac spines. The vertical (infero-superior) axes of the ROI were centred on the line joining the superior iliac spines. The DA was then calculated for the ROI by measuring the ratio of the primary and secondary orientation of trabecular tissue (Whitehouse, 1974; Harrigan & Mann, 1984; Odgaard, 1997; Odgaard et al. 1997; Smit et al. 1998). Specifically, the main and perpendicular trabecular orientations were calculated by analysing radiographic texture, i.e. spatial variation in pixel grey values.

The texture bears an indirect relationship to the bony architecture, such that variation in brightness describes the location of bone to non-bone, i.e. trabecular pattern and orientation (Caligiuri et al. 1993). Radiographic texture was assessed

Table 2 Digitised external (cortical) and internal (trabecular) landmarks are tabulated. Letters M and L denote landmarks from the medial and lateral aspects of the ilium, respectively. Three landmark types were designated following Bookstein (1991). Type I landmarks are located at discrete juxtapositions of bones or bony eminences. Type II landmarks are defined geometrically, for example the apex of an anatomical curve. Type III landmarks are also defined geometrically by chords or fractions of curvature.

No.	Landmark name	Description	Landmark type
External landmarks			
C1	Anterior superior iliac spine		I
C2	Anterior thickening of iliac crest ^M	Point at widest section of anterior iliac crest, between tubercle and superior spine	II
C3	Anterior thickening of iliac crest ^L	Point at widest section of anterior iliac crest, between tubercle and superior spine	II
C4	Iliac tubercle ^M	Point along iliac crest opposite L5	III
C5	Iliac tubercle ^L	Maximum apex of tubercle	II
C6	Iliac crest ^M	Point along medical aspect of iliac crest where the insertion of <i>m. obliquus internus abdominis</i> and <i>m. quadratus lumborum</i> meet	II
C7	Iliac crest ^L	Point along medical aspect of iliac crest where the insertion of <i>m. obliquus externus abdominis</i> and <i>m. latissimus dorsi</i> meet	II
C8	Spina limitans ^M	Point along iliac crest where spina limitans meets iliac crest	II
C9	Lateral iliac crest (Spina limitans) ^L	Lateral aspect of iliac crest opposite L8	III
C10	Posterior eminence of iliac crest ^M	Point at widest section of posterior iliac crest	II
C11	Posterior iliac crest ^L	Point at widest section of posterior iliac crest	II
C12	Posterior superior iliac spine		I
C13	Posterior inferior iliac spine		I
C14	Greater sciatic notch	Deepest point of greater sciatic notch	II
C15	Dorsal ilium	Point along ischial spine where the ilium and ischium meet	II
C16	Lateral apex of acetabular rim		II
C17	Ilio-pubic eminence	The lateral border of the pelvic inlet where the ilium and pubis meet	I
C18	Anterior inferior iliac spine		I
C19	Posterior apex of auricular surface		II
C20	Posterior indent of auricular surface		II
C21	Posterior ridge of auricular surface	Ridge posterior to C16	II
C22	Superior auricular surface	Superior apex of auricular surface	II
C23	Anterior ridge of auricular surface	Ridge anterior to C16	II
C24	Anterior apex of auricular surface	Anterior apex of auricular surface	II
C25	Scalenion	Scalenion	II
C26	Inferior auricular surface	Inferior apex of auricular surface	II
Internal landmarks			
T1	Superior aspect of sacro-pubic bundle	Point where anterior bundle reaches iliac crest	I
T2	Central apex sacro-pubic bundle	Point where anterior bundle reaches acetabulum	I
T3	Inferior aspect of sacro-pubic bundle	Point where posterior bundle reaches iliac crest	I
T4	Superior aspect of ilio-ischial bundle	Central apex of posterior bundle	I
T5	Inferior aspect of ilio-ischial bundle	Point where posterior bundle reaches acetabulum	I

following Russ' (1994) method of creating 2D Fast Fourier Transforms. This technique produces transformed ROIs (complex arrays) with a bright ellipse in the middle (i.e. high grey values) and a dark border (i.e. low grey values; Fig. 2). The eccentricity of the ellipse describes the main and perpendicular directions and the relative amount of bone distributed along the axes. Low eccentricity denotes isotropy, whereas high values indicate anisotropy (Russ, 1994).

To test the repeatability of the DA measures, 10 ilia representing the full age and size range were measured repeatedly, 10 times over 10 days, whereby the order in which the specimens were measured was randomised daily. The percentage error of the DA measurements did not exceed 5%. The measures were

therefore deemed suitable for the study. The DAs in the sacro-pubic and ilio-ischial bundles were compared within developmental stages using a paired *t*-test (Fig. 2). Because there are two independent variables, however, a two-way ANOVA was performed. This test was used to determine whether anisotropy varied significantly between: (i) developmental stages; and/or (ii) across bundles; and whether (iii) there was an interaction between any of the two factors (Table 3). The statistical tests were carried out using PAST version 1.91 (Hammer et al. 2001).

Gross iliac morphology, both cortical and trabecular, was quantified using landmark-based Geometric Morphometric methods. Twenty-nine iliac landmarks, 24 cortical and five trabecular, were digitised (Fig. 1B; Table 2). The cortical land-

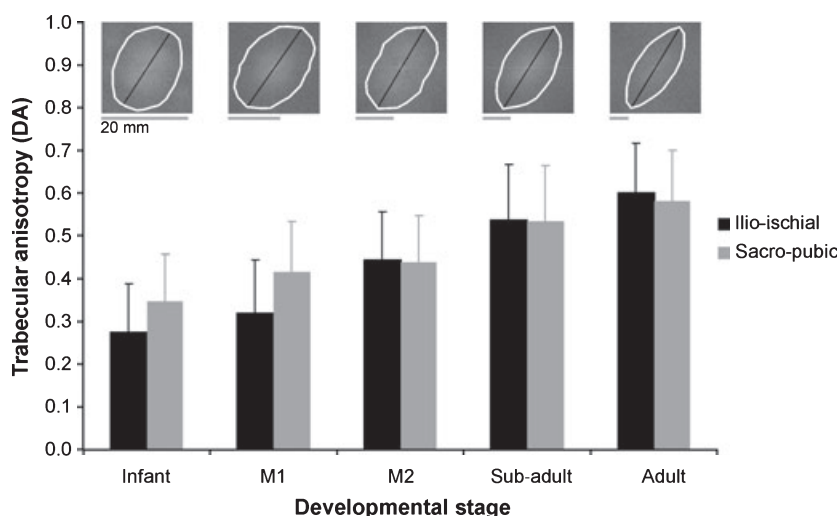


Fig. 2 Ontogenetic variation in mean value and standard deviation in iliac trabecular anisotropy are shown for the sacro-pubic and ilio-ischial bundle, respectively. The typical change in anisotropy in the ilio-ischial bundle is illustrated at the top of the graph by rose plots (white ellipse).

Table 3 Descriptive statistics of iliac trabecular anisotropy in relation to developmental stages and bundle. Mean anisotropy varied statistically significantly among developmental stages; Tukey's *post hoc* test revealed that this result is due to differences between sub-adults/adults and younger developmental stages, respectively. The independent variables were not found to affect each other.

ROI	Infant n = 15		M1 n = 15		M2 n = 10		Sub-adult n = 10		Adult n = 23		Tukey's <i>Post Hoc</i> (Infant vs.)								
	\bar{x}	SD	\bar{x}	SD	\bar{x}	SD	\bar{x}	SD	\bar{x}	SD	F	P	M1	M2	Sub-adult	Adult			
Ilio-ischial	0.27	0.11	0.32	0.12	0.44	0.11	0.54	0.13	0.60	0.12	Developmental Stage	14.15	< 0.0001	0.5668	0.0069	< 0.0001	< 0.0001		
Sacro-pubic	0.35	0.11	0.42	0.12	0.44	0.11	0.53	0.12	0.58	0.12								2.43	0.1200
Overall																		0.81	0.5226
											Interaction								

marks characterised the iliac crest, sciatic notch, caudal ilium, anterior iliac border and auricular surface. Radiographic landmarks characterised the sacro-pubic and ilio-ischial trabecular bundles (see Correnti, 1955; Macchiarelli et al. 1999). Three landmark types were designated following Bookstein (1991). Type I landmarks are located at discrete juxtapositions of bones or bony eminences. Type II landmarks are defined geometrically, for example the apex of an anatomical curve. Type III landmarks are also defined geometrically by chords or fractions of curvature. Only a few of the cortical landmarks, particularly type I, could be accurately located on radiographs. Hence, the points were digitised directly from the ilia in 3D using a Microscribe (model 3DX; Immersion, San Jose, CA, USA), whilst trabecular landmarks were digitised from radiographs in 2D using TPSDig v1.27 (Rohlf, 2004). Three external landmarks were collected from the radiographs also (i.e. the superior iliac spines and the posterior apex of the auricular surface) to facilitate the bone (cortical) and radiographic (trabecular) landmark data sets to be superimposed, for the 3D landmarks to be converted to 2D landmarks, and for the two datasets to be combined by Procrustes fitting.

Geometric Morphometric methods rely on the accurate identification and quantification of landmarks on biological specimens.

Assessing the accuracy of landmark measurements is problematic because of the 'Pinocchio effect' (Cramon-Taubadel et al. 2007), where the superimposition of landmark configurations causes variance of individual landmarks to be spread across all landmarks (Zelditch et al. 2004). Several methods for assessing the accuracy and repeatability of landmark data have been suggested (see Corner et al. 1992; Singleton, 2002; Cramon-Taubadel et al. 2007). Although each of the methods may produce reasonable estimates of measurement error, all require either a constant frame of reference and/or superimposition of configurations. In order to avoid these steps, the accuracy of co-ordinate data was assessed here by comparing digitised inter-landmark distances with measurements collected using calipers (Mitutoyo Digimatic), which do not require Procrustes superimposition. The same 10 specimens used for the DA measurement error test were analysed 10 times on 10 separate days, in a random order. Thirty-six dimensions were measured. The percentage error of inter-landmark distances measured using the caliper and Microscribe did not exceed 5%. Furthermore, the mean inter-landmark distances calculated using the Microscribe always fell within one standard error of the value measured with the calipers (see Ulijaszek & Lourie, 1994). Assuming that there was no systematic error in both the caliper and Microscribe data, the measurements can be considered suitable for analyses.

The patterns of ontogenetic variation in morphology were assessed for the external landmarks (Figs 3a and 4) and the combined external and internal morphology (Figs 3b and 5) separately, using principal component analyses (PCA) based on Procrustes-fitted landmark data. The PCAs removed variation in size from the data sets, but not allometric variation in shape. For the combined set the mean iliac shape for each of the five developmental stages was compared using a pairwise permutation test (10 000 iterations) of Procrustes distances between the groups (Klingenberg & Monteiro, 2005). The commonly adopted use of MANOVA (e.g. Rosas et al. 2008) was avoided because the number of specimens in each case was less than the number of landmarks. The shape differences between stages were visualised using wireframes (Figs 4 and 5). All Geometric Morphometric analyses were carried out using MorphoJ (Klingenberg, 2008).

In order to interpret the ontogenetic allometries within a broader context, Gompertz curves were fit to the PCI scores vs. centroid size, and were compared with the growth standards presented by the National Center for Health Statistics (2000). These results are for interpretation only, and are illustrated in Fig. 6.

Results

Trabecular anisotropy throughout development

Figure 2 shows the mean DA at five developmental stages. The trabecular tissue in infants is relatively isotropic, whilst that of adults is highly anisotropic. At M1 the difference in

anisotropy between the sacro-pubic and the ilio-ischial region approaches statistical significance ($t = 2.148$; $P = 0.051$), with the posterior strut being slightly more anisotropic than the anterior bundle. However, when the interaction between age, position of bundles and DA is assessed within a two-way ANOVA, only the degree of overall anisotropy (anterior and posterior strut) was found to differ between developmental stages (Table 3). Specifically, the DA increases statistically significantly at about M2 eruption (Fig. 2; Table 3).

Ontogenetic shape changes in the iliac cortex

The PCA morphospace in Fig. 3a describes ontogenetic variation in the shape of the iliac cortex. The first two components account for 43% of the total variance. Along PCI, which is correlated with centroid size (quadratic regression coefficient $R^2 = 0.79$), specimens are arranged according to developmental stage. Hence, PCI effectively represents an allometric model of ontogenetic shape change of the modern human ilium. Subsequent PCs, i.e. PCIII–PCVI all account for more than 5% of the variation each, but exhibit no discernible ordering of specimens with respect to developmental stage, population or sex; their biological significance thus remains unclear and these components are therefore not shown. As regards PCII, it is noteworthy that variation

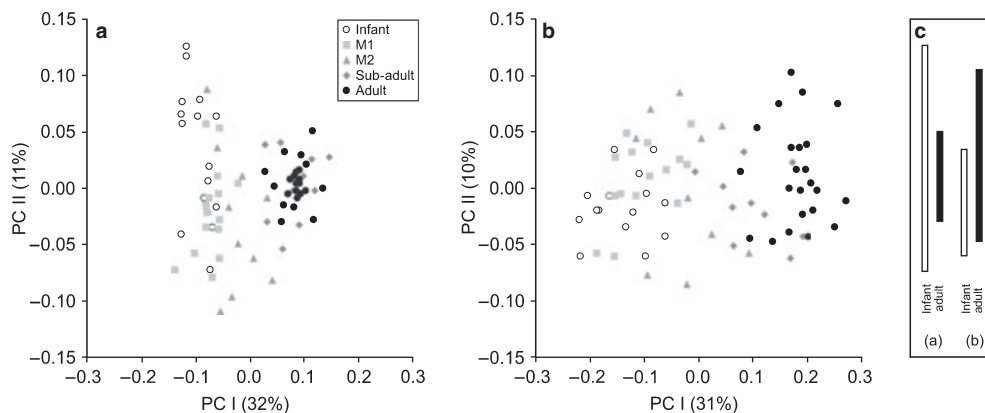


Fig. 3 The first two components of the PCA for (a) external and (b) external and internal landmarks, separately. (c) The difference in variation between infants and adults along PCII is projected into a separate panel to illustrate the decrease and increase of variation with age for external (a) and combined (b) PCA, respectively.

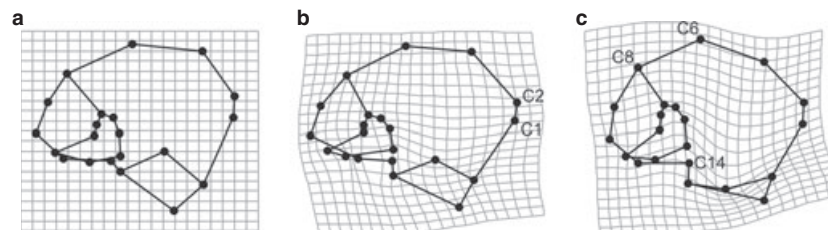


Fig. 4 Procrustes-fitted wireframes and thin-plate splines describing the ontogeny of external iliac shape between growth stages from (a) infancy, (b) eruption stage M2 and (c) adults. Landmarks discussed in the text are shown.






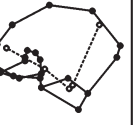



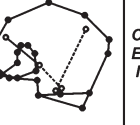




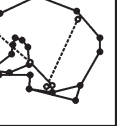
	Infant	M1	M2	Sub-adult	Adult
Infant		<i>C</i> 0.0786 (0.0171) <i>E</i> 0.0694 (0.0319) <i>I</i> 0.0663 (0.0800)	<i>C</i> 0.1030 (0.0025) <i>E</i> 0.0940 (0.0044) <i>I</i> 0.0856 (0.1162)	<i>C</i> 0.1871 (<0.0001) <i>E</i> 0.1626 (<0.0001) <i>I</i> 0.2119 (<0.0001)	<i>C</i> 0.1994 (<0.0001) <i>E</i> 0.1791 (<0.0001) <i>I</i> 0.2414 (<0.0001)
M1			<i>C</i> 0.0824 (0.0621) <i>E</i> 0.0816 (0.0235) <i>I</i> 0.0843 (0.2167)	<i>C</i> 0.1836 (<0.0001) <i>E</i> 0.1661 (<0.0001) <i>I</i> 0.1817 (0.0006)	<i>C</i> 0.1945 (<0.0001) <i>E</i> 0.1769 (<0.0001) <i>I</i> 0.2103 (<0.0001)
M2				<i>C</i> 0.1535 (0.0003) <i>E</i> 0.1359 (0.0001) <i>I</i> 0.1363 (0.0482)	<i>C</i> 0.1663 (<0.0001) <i>E</i> 0.1509 (<0.0001) <i>I</i> 0.1600 (0.0054)
Sub-adult					<i>C</i> 0.0587 (0.1925) <i>E</i> 0.0523 (0.5874) <i>I</i> 0.0536 (0.0803)
Adult					

Fig. 5 Pair-wise comparisons of Procrustes-fitted wireframes of mean developmental stages using both external and internal iliac landmarks. The Procrustes distances between mean specimens and the *P*-values for the permutation test of pairwise distances between the groups are also given for the combined data set (*C*), external landmarks (*E*) and internal strut data points (*I*).

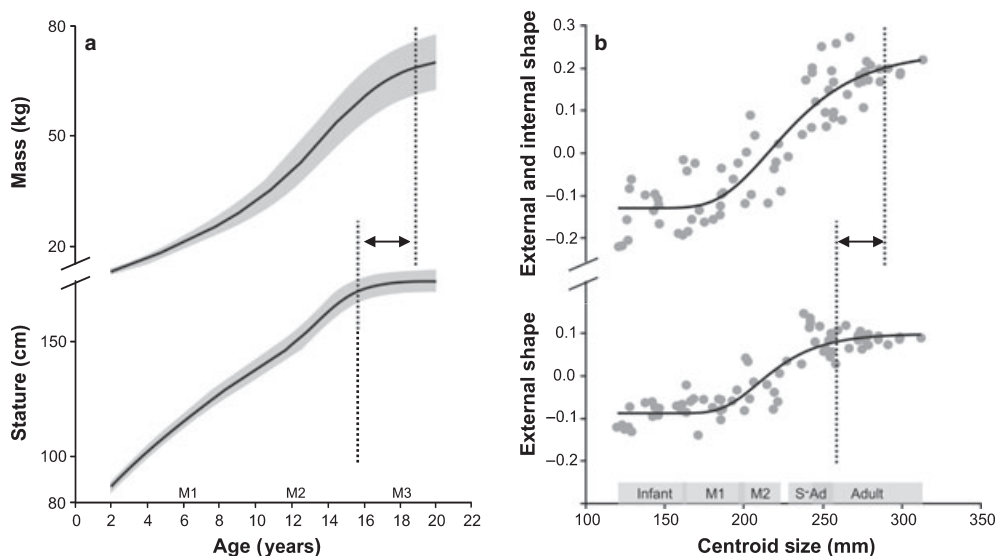


Fig. 6 (a) Growth curves, and 25th percentiles, for male body mass (top) and stature (bottom) (National Center for Health Statistics, 2000) are compared with (b) Gompertz curves for the results of the PCA in Fig. 3. The approximate times for molar eruption are indicated. The PCI scores for combined external and internal landmarks (top) and external landmarks only (bottom) were plotted against centroid size. Developmental stages are denoted at the bottom of the graph. The upper inflection points of the growth curves are highlighted (dashed line), and indicate later cessation of growth for mass than stature (a) and for combined external and internal morphology when compared with external shape alone (b).

decreases as the specimens get older, i.e. infants and juveniles are more variable in outer morphology than adults; this is contrary to the combined analyses of internal and external morphology (Fig. 3b).

From the PCA morphospace two distinct growth stages/patterns seem apparent, as illustrated in Fig. 4. These stages encompass infants to M2, on the one hand, and M2 to adulthood, on the other. Thin-plate splines representing iliac shapes of infants (initial stage), M2 (transitional stage) and adults (final stage) reveal differences in morphology between these apparently distinct developmental stages. Between infancy and M2, the anterior iliac crest (C1, C2) expands anteriorly in relation to the other dimensions of the iliac crest. Between M2 and adulthood, morphological changes mainly concern the posterior and superior aspects of the ilium. Specifically, height at C6 and C8 increases. The auricular surface narrows antero-posteriorly and becomes relatively elongated cranio-caudally, while the sciatic notch (C14) becomes fully established.

Ontogenetic changes in strut orientation in relation to the iliac cortex

Figure 3b shows the first two PCs for the combined data set representing iliac trabecular bundle orientation and iliac cortex. Similar to the analyses of external landmarks alone, PCI and PCII account for just over 40% of the total variance. The quadratic regression coefficient between PCI and centroid size is $R^2 = 0.80$. Similar to cortical analyses, PCIII–VI account for more than 5% of the variation each, but do not reveal any meaningful biological information. Unlike cortical shape, however, variation along PCII increases from younger to older specimens (Fig. 3b); differences in PCII variation between the PCAs are highlighted in Fig. 3c.

The patterns of ontogenetic changes are further explored in Fig. 5 using pairwise comparisons between stages. Throughout development, the sacro-pubic bundle appears to straighten out, such that the acute angle formed between landmarks T1, T2 and T3 increases to almost 180°, and the strut becomes more vertically oriented. This seems to occur in accord with changes in the iliac cortex, such that the sacro-pubic trabecular bundle maintains a constant association with the auricular surface and the acetabulum, which themselves undergo shape changes and cranio-caudal elongation. Conversely, the changes in ilio-ischial bundle position are more complex, whereby the greatest morphological change appears to occur at/after M2 eruption. Specifically, in young adults the position of the bundle becomes more closely aligned with the iliac tubercle (C4). This shift is marked and is reflected in the statistical analyses: the Procrustes distance separating the M2 and sub-adult stages was approximately twofold higher than any other pair of successive growth stages (Fig. 5).

Finally, a significant modification occurs during ontogeny with regard to the inferior position of the trabecular

bundles. While the inferior origins of both bundles are positioned in parallel during early stages of development, they progressively converge and, at about M2/sub-adult stage, they cross over and form the trabecular chiasma. This dense region of iliac trabecular tissue behind the acetabulum is commonly regarded functionally important (e.g. Martinon-Torres, 2003).

Discussion

The present study builds on recent research that highlights the complex nature of trabecular development. On the one hand, it is evident that the textural properties of trabeculae (at least in the ilium) are well defined even prior to the onset of locomotor-related loading (Volpato, 2008; Cunningham & Black, 2009a,b). On the other hand, it is generally assumed that trabeculae exhibit a greater potential for remodelling throughout life (Frost, 1990; Lieberman, 1996; Huiskes, 2000; Carter & Beaupré, 2001; Kobayashi et al. 2003). The two propositions are not necessarily contradictory, however. First, the greater potential for (re)modelling need not apply to early developmental stages, where cortical bone was found to respond plastically to loading too (Lieberman et al. 2003). Second, even if rates of (re)modelling are higher for trabeculae than for compact bone throughout life, this need not affect the basic trabecular bundle arrangement, but may only influence its microstructural properties, such as anisotropy, trabecular thickness, connectivity and spacing, etc. Indeed, an experimental study revealed changes in trabecular orientation to occur only to a limited extent, while other aspects of trabecular organisation, e.g. thickness and spacing, changed statistically significantly in response to altered loading directions (van der Meulen et al. 2006). This pattern of change appears similar to compact bone remodelling which, although resulting in limited changes in external dimensions once adulthood has been reached, still exhibits considerable microstructural changes (e.g. McFarlin et al. 2008). From these previous studies it is parsimonious to conclude that both the shape of the ilium (Lovejoy et al. 1999) and the internal trabecular bundle arrangement within are largely genetically influenced. It is expected that both trabeculae and overall bone shape probably respond in synchrony to mechanical loads during ontogeny (e.g. Ruff et al. 2006), but that microstructural properties may continue to change in a way that can be determined non-invasively, and after the adult shape has been attained. In part, these predictions are borne out by the present study, although some unexpected results were also obtained.

Before interpreting the findings it must be stressed that this is a cross-sectional ontogenetic study of modern human ilia. The bones are derived from different collections and time periods (Table 1), and it must therefore be considered that population differences and secular trends may have influenced the results. While sample sizes are too small to

explore these possibilities further, it is noteworthy in this regard that no obvious trends were revealed by the PCA. Furthermore, insufficient documentation of sex in non-adults confounds an appraisal of the effects of sex on growth patterns, e.g. the sciatic notch (see results shown in Fig. 4). However, of the sexed adult/sub-adult specimens, 16 were classified male and 17 were female. In other words, there is an equal sex ratio in each of the older age categories, and the results can therefore not be attributed to a systematic sex bias in one of these categories. Although ilia are relatively flat and are therefore suitable for such simplified analyses, it is acknowledged that some information may have been missed, especially for older specimens: the modern human pelvis is characterised by an increase in curvature with age (Berge, 1998; Williams & Orban, 2007). Despite these numerous limitations, both sample sizes and the power of the statistical tests employed appear sufficient to draw general conclusions. Importantly, they also allow novel hypotheses to be generated and to help assess the potential for reconstruction of the form–function complex in fossils.

In accord with previous reports (Cunningham & Black, 2009a,b), this study confirms that the distinct trabecular bundle orientation in the pelvis is laid down early during ontogeny. During the earliest prenatal developmental stages, the ilium exhibits a general caudo-cranial fan-shaped orientation of trabeculae, which is likely the result of the direction of growth at the iliac crest and tri-iridate cartilage, i.e. differentiating osteoblasts at the epiphyseal plate. Resorption of trabeculae in areas other than the bundles apparently takes place prior to the onset of loading; in our study, the youngest specimen with clearly identifiable trabecular bundles had a recorded prenatal age of 6 months (unpublished data). Such early definition of struts may be species- and/or bone-specific, however. For example, Tanck et al. (2001) reported for *Sus scrofa* that the adult pattern of trabecular alignment (anisotropy) did not develop until about 100 weeks after birth. Conversely, the arched trabecular patterns in the calcaneus of artiodactyls, which correlate strongly with tension and compression stress trajectories (Lanyon, 1974), are already present in the foetus (Skedros et al. 2004, 2007). Further comparative studies are therefore needed to determine the species- and bone-specific timing of trabecular bundle formation. Regardless, for the modern human ilium a predetermined basis for trabecular bundle development seems evident, either through genetic or epigenetic factors (Cunningham & Black, 2010). However, some loading prior to birth cannot be ruled out. Uncoordinated and sporadic muscle contractions have been reported from as early as 11 weeks intra-uterine (Delaere et al. 1992; Delaere & Dhem, 1999; Scheuer & Black, 2000). The forces thus generated would conceivably contribute to the development of well-defined trabecular bundles. Such functional considerations may explain the trend towards a slightly better defined and more aniso-

tropic sacro-pubic trabecular bundle compared with the ilio-ischial bundle during early stages of development (Fig. 2). The sacro-pubic strut constitutes the main line of force transmission from the auricular surface to the acetabulum (Dalstra & Huijkes, 1995; Volpato, 2008). In light of these considerations, it is also unsurprising that the strut retains a constant relationship with the joint surfaces throughout ontogeny and into adulthood (Fig. 5), despite marked changes in external morphology and orientation of the joint surfaces (Figs 4 and 5). In contrast, the ilio-ischial trabecular bundle attains comparable levels of anisotropy only later during ontogeny, while its overall orientation changes with respect to external landmarks during/after adolescence (Fig. 5).

Modern human locomotor behaviour undergoes major modifications from infancy to adulthood. Key stages in locomotor development include the adoption of an upright stance and bipedal locomotion at about 12–14 months (Halleman et al. 2005), and the attainment of kinematically adult patterns of locomotion between 5 and 9 years old (e.g. Sutherland et al. 1980; Chester et al. 2006). Such shifts in positional and locomotor behaviours should coincide with, or be preceded by, morphological changes in the pelvis. Yet, until about adolescence iliac development appears relatively continuous, as evinced by PCA (Fig. 3) and developmental wireframes (Fig. 5). Apparently thus, both internal and external morphology undergo a similar developmental programme and respond in synchrony to whatever changes in loading regimes occur during ontogeny. The relatively late, and seemingly sudden, alignment of the trabecular bundle with the iliac tubercle and anterior iliac buttress is, however, unexpected (Fig. 5); it appears to be the result of the greater potential for modelling of trabecular tissue during later stages of development (and into adulthood perhaps), i.e. once modelling of external bone shape has slowed/ceased.

The anterior iliac buttress is commonly associated with compressive loads applied to the pelvis in bipedal locomotion and corresponds to the line of action of the abductor muscles when laterally balancing the pelvis (e.g. Lovejoy et al. 1973). It is noteworthy, however, that the most substantial increase in muscle mass occurs after the pubertal growth spurt (Tanner & Whitehouse, 1976; Tanner, 1981; Bogin, 1999, 2002), mediated by an increase in growth hormones (Vogl et al. 1993; Styne, 2003) and after linear growth has ceased (Fig. 6a). In other words, cessation of bone growth occurs prior to somatic maturation and attainment of adult weight. This seems to be mirrored by the PCA for external and combined landmarks, when plotted against centroid size (Fig. 6b). Gompertz curves fitted to the data confirm the allometric aspect of PCI and, importantly, indicate that external adult iliac shape is apparently attained before overall iliac morphology is fully developed; the differences in variation with age found along PCIs for external (Fig. 3a) and combined (Fig. 3b) analyses can thus

be explained also. Taken further, the results imply that morphological shape changes observed during late adolescence/early adulthood are mainly borne by the internal structures (Fig. 5). The statistically significant increase in trabecular anisotropy at this age may therefore be no coincidence and probably reflects the necessity for increased weight-bearing (Table 3). Furthermore, it is tentatively concluded that the re-orientation of the ilio-ischial trabecular bundle during later development may be a direct consequence of increases in body mass also. The underlying causes are proposed to be threefold. First, an increase in abductor muscle mass may increase the force applied to the iliac buttress. Second, changes in muscle mass may lead to kinematic changes in gait. The progressive development of the trabecular chiasma during the sub-adult stage could be relevant in this regard. Third, and probably most important, such a substantial increase in muscle tissue and fat will affect the centre of mass. To what extent this is compensated for by postural adjustments is unclear, but it is predicted that any substantial mass increase will have an effect on the individual's positional behaviour (e.g. Pawlowski & Grabarczyk, 2003; Poussa et al. 2005; Whitcome et al. 2007). If confirmed, the poor correspondence between locomotion and trabecular orientation found in recent studies could thus be explained: architectural properties of trabeculae may reflect habitual positional behaviours more reliably than locomotion.

In summary, the present cross-sectional ontogenetic study of modern human ilia demonstrated bone shape and internal trabecular orientation to be predetermined, and to develop in synchrony until about M2 eruption status, i.e. adolescence. After the adolescent growth spurt, cortical dimensions apparently do not change significantly, whereas the internal structures continue to alter their position relative to external landmarks. These findings have implications for an interpretation of locomotor patterns from external dimensions alone (McHenry & Corruccini, 1975; Berge, 1994; Lovejoy et al. 2009) and/or from immature juvenile specimens, especially fossils (Rook et al. 1999).

Acknowledgements

This study was supported by a NERC studentship NER/S/A/2001/06485 and the Leverhulme Trust F/00 569/C to GM. The following institutions kindly granted access to the material: the Leverhulme Centre for Evolutionary Studies, Cambridge; the University of Liverpool; and the University of Bradford.

References

- Agarwal SC, Dimitriu M, Tomlinson GA, et al. (2004) Medieval trabecular bone architecture: the influence of age, sex, and lifestyle. *Am J Phys Anthropol* **124**, 33–44.
- Berge C (1984) Multivariate analysis of the pelvis for hominids and other extant primates: implications for the locomotion and systematics of the different species of australopithecines. *J Hum Evol* **13**, 555–562.
- Berge C (1994) How did the australopithecines walk? A biomechanical study of the hip and thigh of *Australopithecus afarensis*. *J Hum Evol* **26**, 259–273.
- Berge C (1998) Heterochronic processes in human evolution: an ontogenetic analysis of the hominid pelvis. *Am J Phys Anthropol* **105**, 441–459.
- Berge C, Penin X (2004) Ontogenetic allometry, heterochrony, and interspecific differences in the skull of African apes, using 3-dimensional Procrustes analysis. *Am J Phys Anthropol* **124**, 124–138.
- Biewener AA, Fazzalari NL, Konieczynski DD, et al. (1996) Adaptive changes in trabecular architecture in relation to functional strain patterns and disuse. *Bone* **19**, 1–8.
- Bogin B (1999) Evolutionary perspective on human growth. *Ann Rev Anthropol* **28**, 109–153.
- Bogin B (2002) The evolution of human growth. In: *Human Growth and Development* (ed. Cameron N), pp. 295–320, Amsterdam: Academic Press.
- Bookstein FL (1991) *Morphometric Tools for Landmark Data: Geometry and Biology*. Cambridge: Cambridge University Press.
- Caligiuri P, Giger ML, Favus MJ, et al. (1993) Computerized radiographic analysis of osteoporosis: preliminary evaluation. *Radiology* **186**, 471–474.
- Carlson KJ, Lublinsky S, Judex S (2008) Do different locomotor modes during growth modulate trabecular architecture in the murine hind limb? *Int Comp Biol* **48**, 385–393.
- Carter DR, Beaupré GS (2001) *Skeletal Function and Form: Mechanobiology of Skeletal Development, Aging, and Regeneration*. Cambridge: Cambridge University Press.
- Chester VL, Tingley M, Biden EN (2006) A comparison of kinetic gait parameters for 3–13 year olds. *Clin Biomech* **21**, 726–732.
- Corner BD, Lele S, Richtsmeier JT (1992) Measuring precision of three-dimensional landmark data. *J Quant Anthropol* **3**, 347–359.
- Correnti V (1955) Le basi morfomeccaniche della struttura dell'osso iliaco. *Riv Antrop* **42**, 289–336.
- Cramon-Taubadel N, Frazier BC, Lahr M (2007) The problem of assessing landmark error in geometric morphometrics: theory, methods, and modifications. *Am J Phys Anthropol* **134**, 24–35.
- Cunningham CA, Black SM (2009a) Development of the fetal ilium – challenging concepts of bipedality. *J Anat* **214**, 91–99.
- Cunningham CA, Black SM (2009b) Anticipating bipedalism: trabecular organization in the newborn ilium. *J Anat* **214**, 817–829.
- Cunningham CA, Black SM (2010) The neonatal ilium – metaphyseal drivers and vascular passengers. *Anat Rec* **293**, 1297–1309.
- Dalstra M, Huiskes R (1995) Load transfer across the pelvic bone. *J Biomech* **28**, 715–724.
- Delaere O, Dhem A (1999) Prenatal development of the human pelvis and acetabulum. *Acta Orthop Belg* **65**, 255–260.
- Delaere O, Kok V, Nyssen-Behets C, et al. (1992) Ossification of the human fetal ilium. *Acta Anat* **143**, 330–334.
- Fajardo RJ, Müller R, Ketcham RA, et al. (2007) Nonhuman anthropoid primate femoral neck trabecular architecture and its relationship to locomotor mode. *Anat Rec* **290**, 422–436.
- Frost HM (1990) Skeletal structural adaptations to mechanical usage (SATMU): 2. Redefining Wolff's Law: the remodeling problem. *Anat Rec* **226**, 414–422.

- Gefen A, Seliktar R (2004) Comparison of the trabecular architecture and isostatic stress flow in the human calcaneus. *Med Eng Phys* **26**, 119–129.
- Goldman HM, McFarlin SC, Cooper DML, et al. (2009) Ontogenetic patterning of cortical bone microstructure and geometry at the human mid-shaft femur. *Anat Rec* **292**, 48–64.
- Gosman JH, Ketcham RA (2009) Patterns in ontogeny of human trabecular bone from SunWatch village in the Prehistoric Ohio Valley: general features of microarchitectural change. *Am J Phys Anthropol* **138**, 318–332.
- Hallems A, de Clercq D, Otten B, et al. (2005) 3D joint dynamics of walking in toddlers. A cross-sectional study spanning the first rapid development phase of walking. *Gait & Posture* **22**, 107–118.
- Hammer Ø, Harper DAT, Ryan PD (2001) Past: paleontological statistics software package for education and data analysis. *Palaeontol Electronica* **4**, 9.
- Harrigan TP, Mann RW (1984) Characterization of microstructural anisotropy in orthotropic materials using a second rank tensor. *J Mater Sci* **19**, 761–767.
- Hou JC, Salem GJ, Zernicke RF, et al. (1990) Structural and mechanical adaptations of immature trabecular bone to strenuous exercise. *J Appl Physiol* **69**, 1309–1314.
- Huiskes HWJ (2000) If bone is the answer, then what is the question? *J Anat* **197**, 145–156.
- Ivanenko YP, Dominici N, Cappellini G, et al. (2005) Kinematics in newly walking toddlers does not depend upon postural stability. *J Neurophysiol* **94**, 754–763.
- Iwamoto J, Yeh JK, Aloia JF (1999) Differential effect of treadmill exercise on three cancellous bone sites in the young growing rat. *Bone* **24**, 163–169.
- Klingenberg CP (2008) MorphoJ (http://www.flywings.org.uk/MorphoJ_page.htm).
- Klingenberg CP, Monteiro LR (2005) Distances and directions in multidimensional shape spaces: implications for morphometric applications. *Syst Biol* **54**, 678–688.
- Kobayashi S, Takahashi HE, Ito A, et al. (2003) Trabecular minimodeling in human iliac bone. *Bone* **32**, 163–169.
- Lanyon LE (1974) Experimental support for the trajectorial theory of bone structure. *J Bone Joint Surg* **56-B**, 160–166.
- Lieberman DE (1996) How and why humans grow thin skulls: experimental evidence for systemic cortical robusticity. *Am J Phys Anthropol* **101**, 217–236.
- Lieberman DE, Crompton AW (1998) Responses of bone to stress. In: *Principles of Biological Design: the Optimization and Symmorphosis Debate* (eds Weibel E, Taylor C, Bolis L), pp. 78–86. Cambridge: Cambridge University Press.
- Lieberman DE, Pearson OM, Polk JD, et al. (2003) Optimization of bone growth and remodeling in response to loading in tapered mammalian limbs. *J Exp Biol* **206**, 3125–3138.
- Lovejoy CO, Heiple KG, Burstein AH (1973) The gait of *Australopithecus*. *Am J Phys Anthropol* **38**, 757–779.
- Lovejoy CO, Cohn MJ, White TD (1999) Morphological analysis of the mammalian postcranium: a developmental perspective. *Proc Natl Acad Sci USA* **96**, 13 247–13 252.
- Lovejoy OC, Suwa G, Spurlock S, et al. (2009) The pelvis and femur of *Ardipithecus ramidus*: the emergence of upright walking. *Science* **326**, 71.
- Macchiarelli R, Bondioli L, Galichon V, et al. (1999) Hip bone trabecular architecture shows uniquely distinctive locomotor behaviour in South African australopithecines. *J Hum Evol* **36**, 211–232.
- Macho GA, Abel RL, Schutkowski H (2005) Age changes in bone microstructure: do they occur uniformly? *Int J Osteoarchaeol* **15**, 421–430.
- Marchi D, Sparacello VS, Holt BM, et al. (2006) Biomechanical approach to the reconstruction of activity patterns in Neolithic Western Liguria, Italy. *Am J Phys Anthropol* **131**, 447–455.
- Martinon-Torres M (2003) Quantifying trabecular orientation in the pelvic cancellous bone of modern humans, chimpanzees, and the Kebara2 Neanderthal. *Am J Hum Biol* **15**, 647–661.
- McColl DJ, Abel RL, Spears IR, et al. (2006) An automated method to measure trabecular thickness from micro-computed tomographic scans and its applications. *Anat Rec* **288A**, 982–988.
- McFarlin SC, Terranova CJ, Zihlman AL, et al. (2008) Regional variability in secondary remodeling within long bone cortices of catarrhine primates: the influence of bone growth history. *J Anat* **213**, 308–324.
- McHenry HM, Corruccini RS (1975) Multivariate analysis of early hominid pelvic bones. *Am J Phys Anthropol* **43**, 263–270.
- van der Meulen MCH, Morgan TG, Yang X, et al. (2006) Cancellous bone adaptation to *in vivo* loading in a rabbit model. *Bone* **28**, 871–877.
- Mori T, Okimoto N, Sakai A, et al. (2003) Climbing exercise increases bone mass and trabecular bone turnover through transient regulation of marrow osteogenic and osteoclastogenic potentials in mice. *J Bone Miner Res* **18**, 2002–2009.
- National Center for Health Statistics (2000) *Stature-for-Age and Weight-for-Age Percentiles 2 to 20 Years: Boys*. [Online] (Updated 21 November 2009). Available at: <http://www.cdc.gov/growthcharts> [Accessed 22 March 2010].
- Odgaard A (1997) Three-dimensional methods for quantification of cancellous bone architecture. *Bone* **20**, 315–328.
- Odgaard A, Kabel J, van Rietbergen B, et al. (1997) Fabric and elastic principal directions of cancellous bone are closely related. *J Biomech* **30**, 487–495.
- Pawlowski B, Grabarczyk M (2003) Center of body mass and the evolution of female body shape. *Am J Hum Biol* **15**, 144–150.
- Pearson OM, Lieberman DE (2004) The aging of Wolff's "law": ontogeny and responses to mechanical loading in cortical bone. *Yrbk Phys Anthropol* **125**, 63–99.
- Penin X, Berge C, Baylac M (2002) Ontogenetic study of the skull in modern humans and the common chimpanzees: neotenic hypothesis reconsidered with a 3-dimensional Procrustes analysis. *Am J Phys Anthropol* **118**, 50–62.
- Pontzer H, Lieberman DE, Momin E, et al. (2006) Trabecular bone in the bird knee responds with high sensitivity to changes in load orientation. *J Exp Biol* **209**, 57–65.
- Poussa MS, Heliovaara MM, Seitsamo JT, et al. (2005) Development of spinal posture in a cohort of children from the age of 11 to 22 years. *Eur Spine J* **14**, 738–742.
- Robson-Brown KA, Davies EN, McNally DS (2002) The angular distribution of vertebral trabeculae in modern humans, chimpanzees and the Kebara 2 Neanderthal. *J Hum Evol* **43**, 189–205.
- Rohlf FJ (2004) tpsDig (<http://life.bio.sunysb.edu/morph/>).
- Rook L, Bondioli L, Köhler M, et al. (1999) *Oreopithecus* was a bipedal ape after all: evidence from the iliac cancellous architecture. *Proc Natl Acad Sci USA* **96**, 8795–8799.
- Rosas A, Bastir M, Alorcón JA, et al. (2008) Thin-plate spline analysis of the cranial base in African, Asian and European

- populations and its relationship with different malocclusions. *Arch Oral Biol* **53**, 826–834.
- Ruff CB** (2005) Mechanical determinants of bone form: insights from skeletal remains. *J Musculoskelet Neuronal Interact* **5**, 202–212.
- Ruff C, Holt B, Trinkaus E** (2006) Who's afraid of the big bad wolff?: "wolff's law" and bone functional adaptation. *Am J Phys Anthropol* **129**, 484–498.
- Russ JC** (1994) *Fractal Surfaces*. New York: Plenum Press.
- Ryan TM, Ketcham RA** (2002) The three-dimensional structure of trabecular bone in the femoral head of strepsirrhine primates. *J Hum Evol* **43**, 1–26.
- Ryan TM, Krovitz GE** (2006) Trabecular bone ontogeny in the human proximal femur. *J Hum Evol* **51**, 591–602.
- Ryan TM, van Rietbergen B** (2005) Mechanical significance of femoral head trabecular bone structure in *Loris* and *Galago* evaluated using micromechanical finite element models. *Am J Phys Anthropol* **126**, 82–96.
- Scheuer L, Black S** (2000) *Developmental Juvenile Osteology*. London: Academic Press.
- Singleton M** (2002) Patterns of cranial shape variation in the Papionini (Primates: Cercopithecinae). *J Hum Evol* **42**, 547–578.
- Skedros JG, Hunt KJ, Bloebaum RD** (2004) Relationships of loading history and structural and material characteristics of bone: development of the mule deer calcaneus. *J Morphol* **259**, 281–307.
- Skedros JG, Sorenson SM, Hunt KJ, et al.** (2007) Ontogenetic structural and material variations in ovine calcanei: a model for interpreting bone adaptation. *Anat Rec* **290**, 284–300.
- Sládek V, Berner M, Sailer R** (2006) Mobility in Central European late Neolithic and Early Bronze Age: Femoral Cross-Sectional Geometry. *Am J Phys Anthropol* **130**, 320–332.
- Smit TH, Schneider E, Odgaard A** (1998) Star length distribution: a volume-based concept for the characterization of structural anisotropy. *J Microsc* **191**, 249–257.
- Studel K** (1982) Patterns of intraspecific and interspecific allometry in Old World primates. *Am J Phys Anthropol* **59**, 419–430.
- Stock J, Pfeiffer S** (2001) Linking structural variability in long bone diaphyses to habitual behaviours: foragers from the southern African Later Stone Age and the Andaman Islands. *Am J Phys Anthropol* **115**, 337–348.
- Styne DM** (2003) The regulation of pubertal growth. *Horm Res* **60**, 22–26.
- Sutherland DH, Olshen R, Cooper L, et al.** (1980) The development of mature gait. *J Bone Joint Surg* **62-A**, 336–353.
- Tanck E, Homminga J, van Lenthe GH, et al.** (2001) Increase in bone volume fraction precedes architectural adaptation in growing bone. *Bone* **28**, 650–654.
- Tanner JM** (1981) Growth and maturation during adolescence. *Nutr Rev* **39**, 43–55.
- Tanner JM, Whitehouse RH** (1976) Clinical longitudinal standards for height, weight, height velocity, weight velocity, and stages of puberty. *Arch Dis Child* **51**, 170–179.
- Ulijaszek SJ, Lourie JA** (1994) Intra- and inter-observer error in anthropometric measurement. In: *Anthropometry: the Individual and the Population* (eds Ulijaszek SJ, Mascie-Taylor CGN), pp. 30–55. Cambridge: Cambridge University Press.
- Vogl C, Atchley WR, Cowley DE, et al.** (1993) The epigenetic influence of growth hormone on skeletal development. *Growth Dev Aging* **57**, 163–182.
- Volpato V** (2008) Morphogenèse de l'endostructure osseuse de l'ilion humain. *C R Palevol* **7**, 463–471.
- Wallace JM, Rajachar RM, Allen MR, et al.** (2007) Exercise-induced changes in the cortical bone of growing mice are bone- and gender-specific. *Bone* **40**, 1120–1127.
- Whitcome KK, Shapiro LJ, Lieberman DF** (2007) Fetal load and the evolution of lumbar lordosis in bipedal hominins. *Nature* **250**, 1075–1078.
- Whitehouse WJ** (1974) The quantitative morphology of anisotropic trabecular bone. *J Microsc* **101**, 153–168.
- Williams FL, Orban R** (2007) Ontogeny and phylogeny of the pelvis in *Gorilla*, *Pongo*, *Pan*, *Australopithecus* and *Homo*. *Folia Primatol* **78**, 99–117.
- Wolff J** (1892) *Das Gesetz der Transformation der Knochen*. Berlin: Verlag von August Hirschwald.
- Zelditch ML, Swiderski DL, Sheets HD, et al.** (2004) *Geometric Morphometrics for Biologists: a Primer*. San Diego: Elsevier Academic Press.